Journal of Control Science and Engineering 2 (2014) 61-69

# Indoor Narrowband Power Lines Channel Characterization

Anouar Achouri[1, 2], Jean-Charles Le Bunetel[2], Yves Raingeaud[2] and Richard Nizigiyimana[2]

*1. LAN (Laboratoire des Applications Numérique) Digital Lab, Tauxigny 37165, France*

*2. GREMAN (Research Group on Materials, Microelectronics, and Acoustics Nanotechnology), University of Tours, Tours 37200, France*

**Abstract:** Power line is an efficient media for home area networking communication scenarios. However, it is not designed to transmit data. This causes several perturbations phenomenon for communications technologies over the power cables. This work presents an investigation of the indoor narrowband power lines channel behavior. The load, the transmission line length and the network topology impact are studied using a simple network. A channel response measure campaign has been realized in 13 sites. The channel capacity has been used for channel classification. The measures were classified into 5 classes. It is shown that channel response is mainly impacted by the load impedance. The class distributions are more impacted by the nature of appliances connected into the indoor network.

**Key words:** Power lines channel, narrowband, load impedance, channel classification.

## 1. Introduction

The low cost and the implementation simplicity aspects of the narrowband power lines communication technology promotes it among DSOs (distribution system operators). Many DSOs and electric utilities have opted for narrowband power lines solutions in the recent past, such as ERDF (Electricité Réseau Distribution France) for G3-PLC (power lines channel) [1] and IBERDROLA for PRIME [2] to ensure the command of the power grid and the remote smart metering in real time beyond smart grid applications.

Currently, such technologies address mainly outdoor & grids applications and do not take part in indoor scenarios, such as control and command of household appliances. The use of narrowband PLC systems for home automation is evoked in the emergent narrowband PLC standard IEEE (Institute of Electrical and Electronics Engineers) 1901.2 and in the G.hnem technology [3] which addresses both indoor and outdoor communications. The indoor Smart Grid applications are currently geared towards improving the indoor energy efficiency, reducing the power peak consumption, and balancing power demand and production using electrical vehicles as energy suppliers [4]. Power lines is also an adequate media for others home applications like electric vehicle to charging station communication, and home area networking communications scenarios [5, 6].

However, this transmission support is basically designed for power transit not for HF (high frequency) communications. Many studies have been realized to characterize high frequencies (frequencies above 1 MHz) power lines channel [7-9]. Many power lines characteristics could disturb the communication over power lines. In Ref. [10] and Ref. [12], the frequency selectivity of the PLC channel is emphasized. It consists of fadings at particular frequencies. This could be explained by the multipath carried by signals transmitted in the channel Ref. [7]. In Ref. [9], PLC channel is modeled using an equation describing the multipath behavior of the channel. PLC channel is

**Corresponding author:** Anouar Achouri, Ph.D. student, research fields: transmission lines, communication power line, smart grid, electromagnetic compatibility. E-mail: anouar.achouri@gmail.com.

time varying due to the connection and the disconnection of the loads and/or the line segments Ref. [12, 13]. The power lines channel in the FCC, ARIB and Cenelec bands Ref. [14] is not sufficiently investigated. Few studies about the narrowband indoor power line channels are presented in the literature. Some studies have treated the channel attenuations variations with frequency, distance, time and location as well as the presence of frequency selective fading [15, 16]. A statistic study about the coherence bandwidth and the channel capacity is performed in Ref. [17].

In this work, the indoor power lines communications is studied in the band (9 kHz-500 kHz). In this band, the power lines channel behavior is largely impacted by the connected appliances behavior. In the first part of this article, the load impedance impact on channel is investigated. The study is carried out by using a simple electrical network topology to determine the load impedance, the load position and the network topology impact on the channel response behavior. In the second part, the results of the power lines channel measure campaign are exposed. This campaign consists of more than 10,000 channels transfer functions measured in 13 different sites. A performance based classification and a statistical study of the channel response are presented at the end of this work.

## 2. Channel Characterization Using Known Loads

### *2.1 Measurements Set-up*

This section outlines the measure scheme of the channel response using a T-network (Fig. 1). The measurements are reported in presence of a typical load (capacitive, inductive and resistive) at several positions in the T-network (P1, …, P5). Channel transfer functions are carried out by means of a vector network analyzer. The test set-up is calibrated by an electronic calibration kit.

### *2.2 Loads Characteristics*

In Fig. 2, the impedance characteristics of a capacitive $C_2$ and an inductive $L_2$ loads with high impedance are represented. In Fig. 3, the curve with solid line represents the inductive load $L_1$ with low impedance and the curve with dashed line represents the capacitive load $C_1$ with low impedance. This last load exhibits an inductive behavior for frequencies superiors of 320 kHz. In addition to these loads, three resistances $R_1$ = 10 Ω, $R_2$ = 50 Ω and $R_3$ = 100 Ω are used in this study.

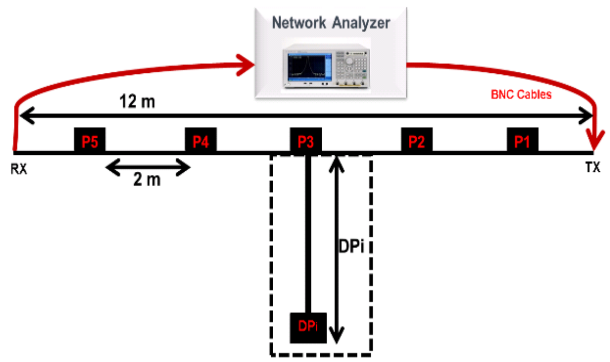


**Fig. 1 Measurements scheme.**

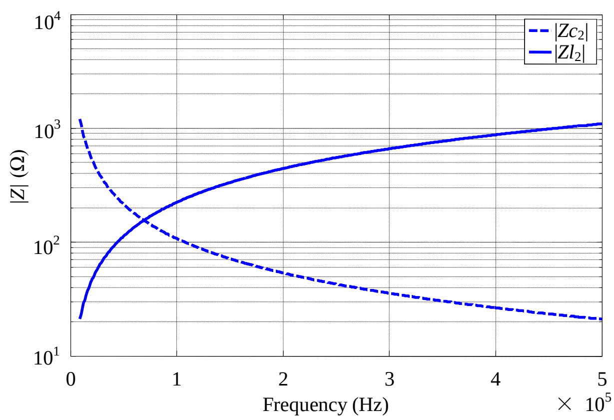


**Fig. 2 High impedance loads characteristics.**

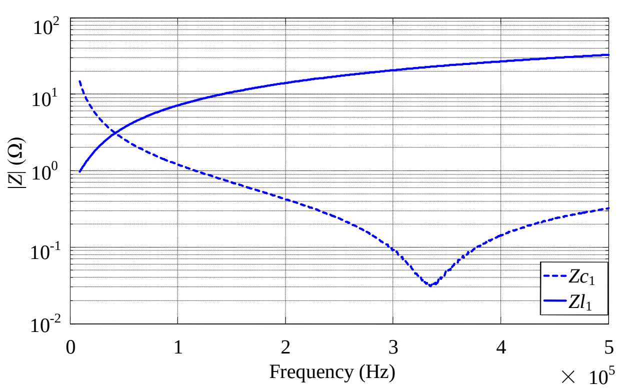

**Fig. 3 Low impedance loads characteristics.**

## *2.3 Channel Characterization Using a Cable without Derivation*

### 2.3.1 Impedance Effect on Channel Response

In this part, the derivation cable is unplugged. The study is carried on within a 10 m cable between the TX and the RX. This configuration is used to study the impedance magnitude effects on channel response. The channel response is reported in presence of a load at P3 outlet (Fig. 1). The Fig. 4-6 represents the transfer function module measurement the $|S_{21}|$ in presence of each load.

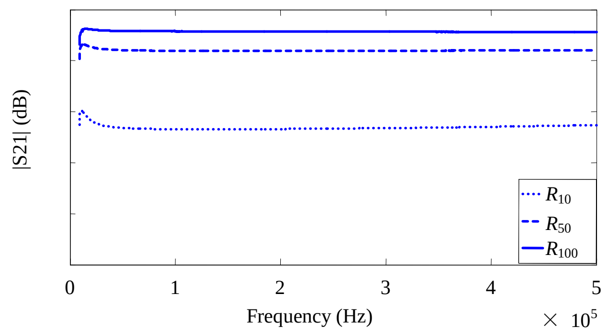


**Fig. 4 Transfer function variations in presence of resistors.**

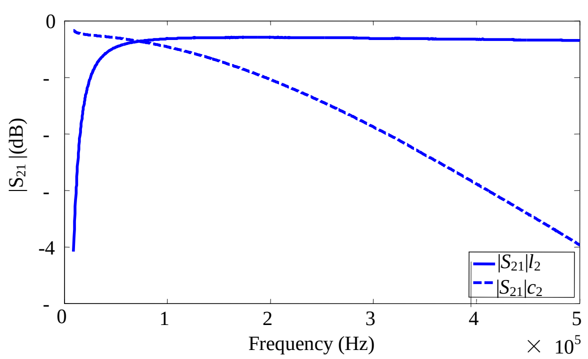


**Fig. 5 Transfer function variation in presence of high impedance loads.**

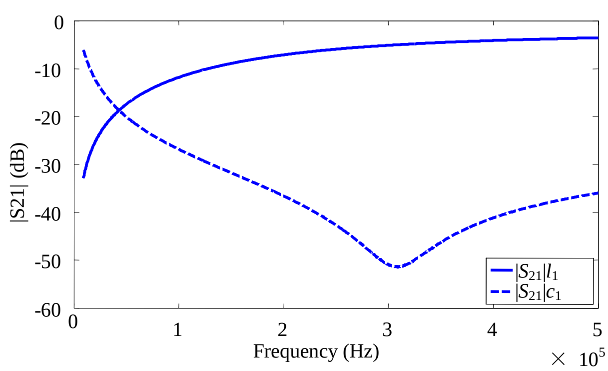


**Fig. 6 Transfer function variation in presence of low impedance loads.**

Two channels characteristics can be distinguished: channel in presence of load with high impedance and channel in presence of load with low impedance. In presence of high impedance load, the channel response has a small attenuation (less than 2 dB for $Z$ = 100 Ω (Figs. 2 and 5)). In presence of load with low impedance, the $|S_{21}|$ function presents a deep attenuation at frequencies with low impedance. The attenuation reaches more than 50 dB when the capacitive load is plugged. As inductive impedance increases with frequency $|Z| = |L|$ and the capacitive impedance decreases with frequency $|Z| = |1/C|$ and at (9 kHz-500 kHz), the inductance $L$ and the capacitance $C$ remain constants, we can observe that the $|S_{21}|$ magnitude increases with frequency in the case of inductive impedance and decreases in the case of capacitive load. The capacitive load used in this experience changes the behavior at 320 kHz and becomes inductive. That explains why the transfer function increases after the frequency of 320 kHz. In the rest of this work, our interest is on poor impedance loads ($R$ = 10 Ω, $L_1$ and $C_1$ in Fig. 4).

### 2.3.2 Loads Positions Impacts on Channel Response

In this part, the transfer function between the TX and the RX is studied in presence of each of the three loads at the several cable outlets. Differences between measured $|S_{21}|$ in presence of inductive and resistive load at the several outlets of the RX-TX cable have not exceeded 0.3 dB (Fig. 7).

### 2.3.3 Channel Response in Presence of Several Loads

The experience consists of plugging a combination of loads in the network. The transfer function variations are reported in Figs. 8-10.

The channel response is dominated by the lower impedance effect. In Fig. 9, the inductive loads effect on channel for the frequencies is lower than 100 kHz. For frequencies greater than 100 kHz, the $|S_{21}|$ reaches asymptotically the transfer function variations measured with the presence of the resistive load. In

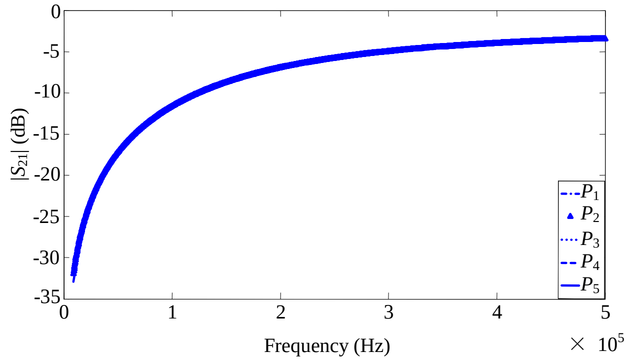


**Fig. 7 Transfer function variation with inductive load at several positions.**

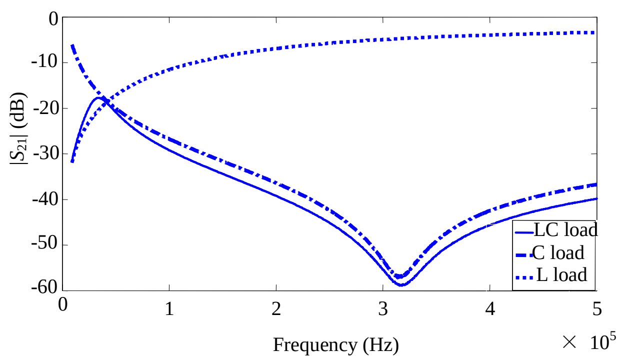


**Fig. 8 Transfer function measurements in presence of LC loads.**

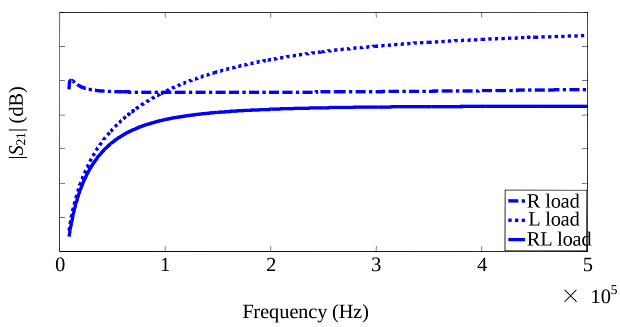


**Fig. 9 Transfer function measurement in presence of RL loads.**

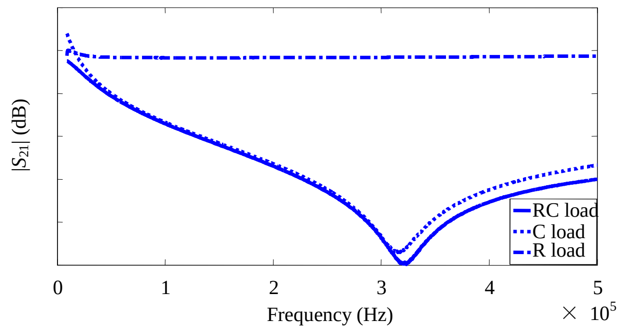


**Fig. 10 Transfer function measurement in presence of RC loads.**

Fig. 8 the | $S_{21}$| variations in presence of the inductive load and the capacitive load is reported. The $|S_{21}|$ behaves like $|S_{21}|$ measured in presence of inductive load in the frequency band (9 kHz-70 kHz) as the inductive impedance is lower than the capacitive impedance in this frequency band. For frequencies superior than 70 kHz, the power line channel behavior is dominated by the capacitive load. The $|S_{21}|$ variations measured in presence of LC load remains below $|S_{21}|$ in presence of $C$ load and in presence of L load except at the resonance frequency of the LC filter, which correspond to $Z_L = Z_C$.

### *2.4 Channel Characterization in Presence of Derivations in the Cable*

In this experience, the effect of the derivation is studied. The experience has begun by the measure of $S_{21}$ with several lengths of derivations and with derivations at several positions and without loads plugged into the network. The measures have shown that there was no channel transfer function attenuation in presence of derivations without loads. To study the impact of loads plugged in derivations, we have plugged a cable at P3 position (Fig. 1). To study the derivation length effect on the channel response, we have used four derivation cables. Each load is plugged at the end of the derivation cable. The used cables lengths $DP_i$ are $DP_1$ = 1 m, $DP_2$ = 4 m, $DP_3$ = 7 m and $DP_4$ = 9 m. To analyze the derivation effect on channel, the load impedance connected into the derivation cable is computed at the derivation connection point using the transmission theory. In Fig. 11, the derivation cable is represented by the *BD* portion. The distance *BD* represents one of the four lengths $DP_1$, $DP_2$, $DP_3$ and $DP_4$.

$$Z_{eq} = Z_c \frac{Z_l + Z_c \tanh(\bar{\gamma} \times l)}{Z_c + Z_l \tanh(\bar{\gamma} \times l)} \quad (1)$$

$$\overline{Z_c} = \sqrt{\overline{Z_{cc}} \times \overline{Z_{co}}} \quad (2)$$

$$\bar{\gamma} = \frac{\tan^{-1}\left(\sqrt{\frac{\overline{Z_{cc}}}{\overline{Z_{co}}}}\right)}{l} \quad (3)$$

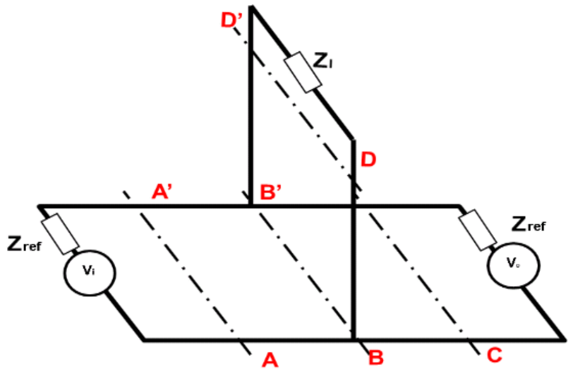


**Fig. 11 Network topology.**

$Z_{eq}$: the load impedance computed at the BB' plan
$Z_c$: the characteristic impedance
$\bar{\gamma}$ : the propagation coefficient
$Z_l$ : the load impedance
$Z_{cc}$ : the short impedance
$Z_{co}$ : the open impedance
*l*: the derivation length

In the Fig. 12, the capacitance impedance computed at BB' plan is represented. The impedance magnitude increases with the derivation length, and the capacitance load exhibits an inductive behavior at frequencies lower than 320 kHz, so it has changed the behavior at 170 kHz for 1 m derivation length, 90 kHz for 4 m derivation length, 75 kHz for 7 m derivation length and 70 kHz for 9 m derivation.

The $|S_{21}|$ measurements in presence of loads at several positions in the derivation cable are presented in Fig. 13 for the resistive load, in Fig. 16 for inductive load and in Fig. 17 for capacitive load. $|S_{21}|$ vary proportionally with the derivation longer. For resistor and inductive loads, the difference has reached about 5 dB at 500 kHz between measured $|S_{21}|$ in presence of load connected at a 9 m derivation length (*BD* = 9 m) and load connected at $P_3$. In presence of the capacitive load at $DP_1$ and at $DP_4$, the difference between measured transfer functions for each case, has reached about 28 dB at 320 kHz. The inductive behavior of $|S_{21}|$ is observed at 170 kHz with 1 m derivation length, at 95 kHz with 2 m derivation length, at 75 kHz with 7 m derivation length and at 70 kHz at 9 m derivation

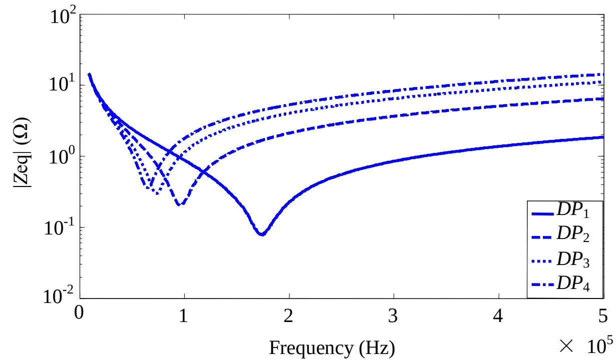


**Fig. 12 Impedance magnitude seen at BB' plan.**

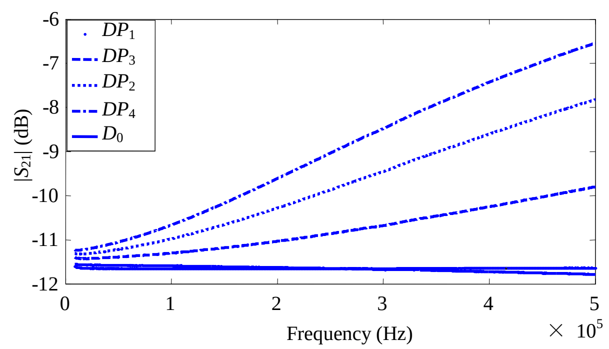


**Fig. 13 Transfer function measurements in presence of resistor loads in cable with derivation.**

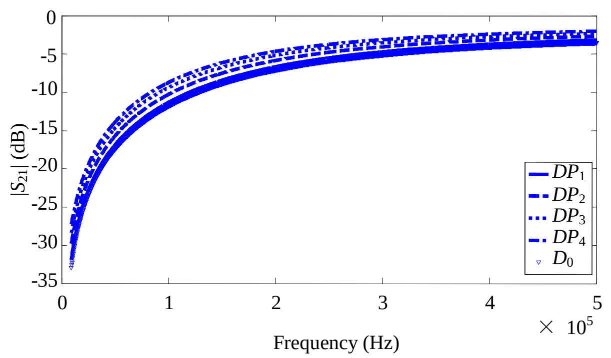


**Fig. 14 Transfer function measurements in presence of inductive loads in cable with derivation.**

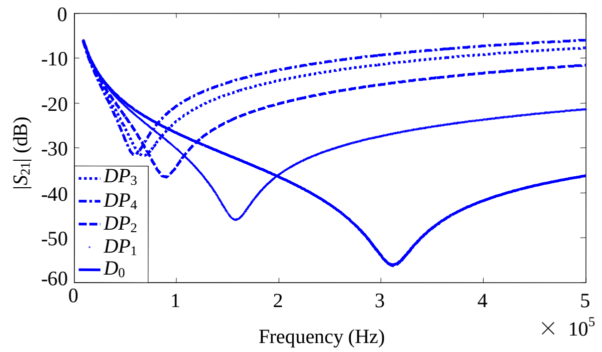


**Fig. 15 Transfer function measurements in presence of capacitive loads in cable with derivation.**

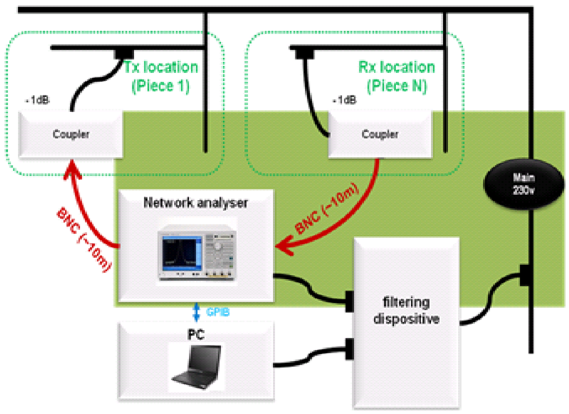


**Fig. 16 Measurements scheme.**

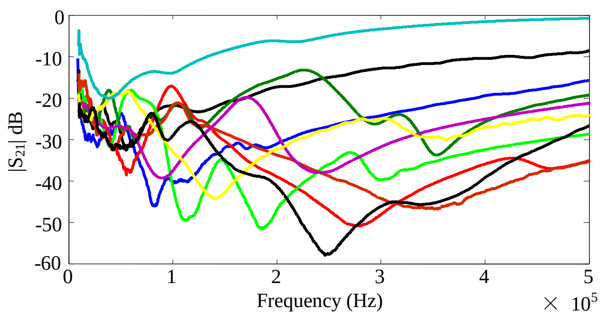


**Fig. 17 TF measurements examples.**

length while it was observed at 320 kHz without derivations. The measured $|S_{21}|$ is homogenous to the relatives computed impedance $|Z_{eq}|$. Every extremum in the impedance magnitude correspond to an extremum in the measured $|S_{21}|$.

## 3. Conclusion

In absence of noises perturbations, the power lines behavior is studied using several scenarios. The narrowband PLC channel attenuation is mainly caused by impedance mismatching and especially in presence of loads with very low impedance. The use of a power off cables and several loads has permitted to give a preliminary idea about the behavior of the power line channel. To extend the study of the indoor power line channel behavior, a measurement campaign has taken place at several indoor sites.

## 3. Domestic PLC Channel Characterization

### *3.1 Measurements Set-up*

The PLC transfer functions are measured between a principle outlet (the nearest one to the electrical meter) and one outlet in another piece of the measure site (kitchen, bedroom and living room). Twenty transfer functions were taken in burst at every two hours. The total number of transfer function measured at the 13 sites is 10220 transfer functions. The table1 presents the sites types, and the TF (transfer functions) number measured in each site.

### *3.2 Observations*

Transfer functions measurements results have shown a similarity between measurements realized at same site (same pace, peaks and notch at the same frequencies). Some differences between channel transfer function could be found between measurements taken at a small time intervals (less than 3 secs of difference between two measures) due to the random behavior of the electrical network impedance. In Fig. 11, transfer functions from several sites are presented. The measured transfer functions are dominated by the inductive load behavior at high frequency ($f$ > 300 kHz). Some of measured transfer channel exhibits a linear variation due to the dominant inductive load effect. Generally, it has less attenuation than other power lines channel. Some measured power lines channel exhibits a complex behavior with many peaks (caused by LC resonance phenomenon) and many notches (caused by LC anti-resonance phenomenon).

**Table 1 Measures sites properties.**

| Site | Number of TF | Site type |
| --- | --- | --- |
| 1 | 960 | A-C-renewed |

| | | |
|---|---|---|
| 2 | 960 | H-C-renewed |
| 3 | 720 | C-renewed |
| 4 | 960 | H-U-old |
| 5 | 720 | H-C-old |
| 6 | 720 | A-U-old |
| 7 | 720 | A-U-old |
| 8 | 600 | H-U-old |
| 9 | 720 | H-U-new |
| 10 | 720 | H-U-new |
| 11 | 720 | H-U-new |
| 12 | 720 | A-U-new |
| 13 | 960 | A-U-old |

C = rural, U = urban, A = apartment, H = house

The distribution of notches and peaks are completely random. It is caused by the great number of appliances connected simultaneously to the indoor power lines network. Based on this random behavior of power lines channel, the measured transfer channel was classified using the channel capacity as a classification parameter. As in Ref. [5] the capacity presents an efficient parameter to distinguish between channels.

### *3.3 PLC Channel Classification*

PLC channels are classified using capacity (according to Shanon's formula) as a classification parameter.

$$C = \Delta f \times \sum_{i=1}^{N} \log_2\left(1 + \frac{P_e \times H(f)^2}{P_n}\right) \text{ (bit/s)} \quad (3)$$

With $\Delta f$ = 306 is the frequency width and $N$ = 1,601 is the carriers number. In Fig. 18, we present the noise power $P_n$ ($P_{n50}$ in dBm/200 Hz) and the transmitter mask $P_e$ ($P_e$ in dBm/200 Hz) is defined by the ITU (the international telecommunication union) in Ref. [2] for the PLC specifications in the FCC band plans.

The noise power was fitted from measured noises and the transmitter mask was defined by the ITU in Ref. [1] for the PLC specifications in the FCC band plans.

The measured channels are classified into five classes. The computed capacity varied between 1.5 Mbps and 7.5 Mbps. In Fig. 19, sample from each class is presented.

Channel with the lowest attenuations had the highest capacities. In Fig. 19, Class 1 (C1) transfer channel magnitude example was above -10 dB, Class 2 (C2) channel magnitude transfer channel was above –15 dB, the Class 3 (C3) example exhibits complex behavior with many peaks and vary between -30 dB and -10 dB, the Class 4 (C4) channel transfer function example had an attenuation lower than Class 2 (C2) channel example in (9 kHz-100 kHz) band and roughly the same attenuation in [350 kHz-500 kHz]

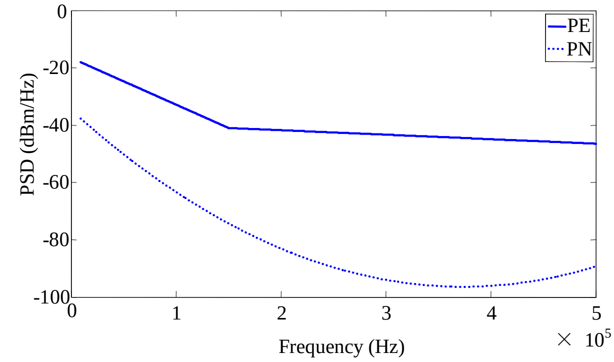


**Fig. 18 Noise and signal PSD.**

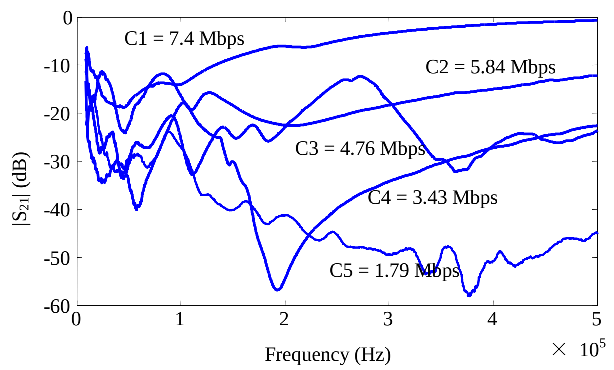


**Fig. 19 Transfer channel examples.**

**Table 2 Class distribution.**

| Class | Percentage |
|---|---|
| 1 | 13.85 % |
| 2 | 8.83% |
| 3 | 33.30% |
| 4 | 23.85% |
| 5 | 20.17% |

frequency band but a deep attenuation in [100 kHz-350 kHz] frequency band reaching - 58 dB and the Class 5 (C5) channel transfer function example magnitude was between －40 dB and －58 dB for frequencies above 100 kHz and between －20 dB and –40 dB for [9 kHz-100 kHz] band.

Table 3 reports the channels distribution by classes. Only 22% of total measured channels had a capacity that exceeds 5 Mbps (Class 1 (C1) and Class 2 (C2) channel) while represents 54% of measured channels had a capacity below 4 Mbps (Class (C4) and Class 5 (C5) channels). The third of channels belongs to the Class 3 (C3) channels.

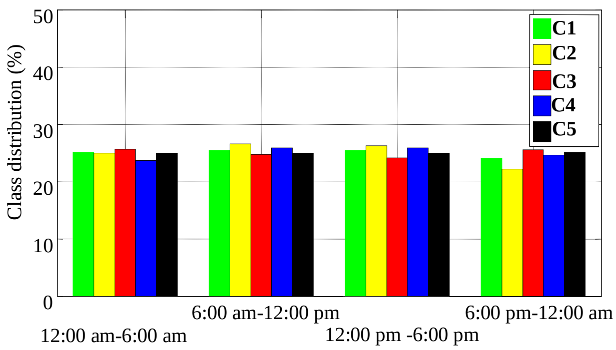


**Fig. 20 Distribution of channel class during the day.**

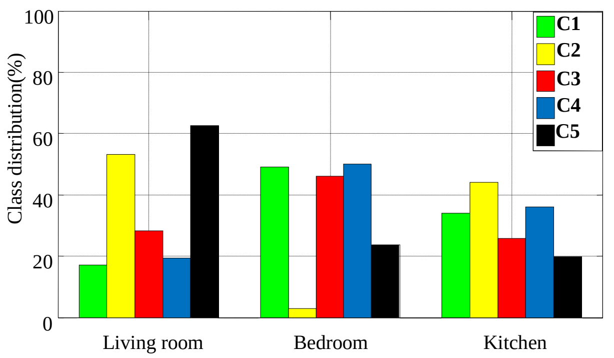


**Fig. 21 Distribution of channels class in the measure piece.**

### *3.4 Classes Distribution Based on Measurement Moment*

The Class 1 (C1) and the Class 5 (C5) channels had a uniform distribution during the four quarts which accentuate the independence of this class channels on time. The rest of channels did not have many distributions variations in time. The Class 2 (C2) has reached its distribution peak in the second day quart, the Class 3 (C3) has reached its distribution peak in the last day quart while the Class 4 (C4) channel was concentrated in the second and the third day quart.

### *3.5 Classes Distribution Based on Measurement Piece Type*

The Class 1 (C1) channels distribution was uniform in function of measure room. The Class 2 (C2) channels distribution has reached its distribution peak in the bedroom distribution, the Class 3 (C3) channels has reached its peak distribution in kitchen, the Class 4 (C4) has reached its distribution peak in the living room and the Class 4 (C4) channel had almost a uniform distribution.

The statistical study shows small variations in the classes' distribution among the measure duration and a more important variation class's distribution between measure rooms. This could be explained by the powerful independence of the channel behavior to the load impedance behavior in rooms. Some channel behavior change is observed during the 24 h measure and it could be resulted of the plug in or the plug out of some electrical appliances. Channel transfer function could also change the curve without changing the class.

## 4. Conclusion

This contribution presents an exploration of the PLC channel in the band (9 kHz-500 kHz). In the first part, the load effect was studied using a simple network. It has been shown that low impedance load attenuates the channel transfer function and the load effect depends not only on its impedance magnitude position but it could also be impacted by its position and its nature. The use of known loads for channel characterization has served us for the indoor power lines channel behavior studying. In the second part of our contribution, we have presented the PLC channel measurement results. The measured channel transfer function founts have exceeded 10,000 samples realized in 13 sites. These transfer function samples were classified using a based performance parameter "channel capacity" factor into 5 Classes. A statistics based on measurement moment and measure piece type was carried out. It has shown that channel performance depends basically on room type in which we have found some important variation (most of class 5 channels was measured in the living room while it had the smallest Class 1 (C1) channel part). The measured transfer channels constitute a data base for a channel emulator. This emulator will generate models from each channel class.

## Acknowledgment

We would like to thanks the LAN laboratory www.lanpark.eu for sponsoring this work

## References


[1] ITU-T G. 9903. Narrow-Band Orthogonal Frequency Division Multiplexing Power Line Communication Transceivers for G3-PLC Networks.

[2] ITU-T G. 9904. 2012. Narrowband Orthogonal Frequency Division Multiplexing Power Line Communication Transceivers for PRIME Networks.

[3] ITU-T G. 9902. Recommendation ITU-T G.9902. 2012. Narrowband Orthogonal Frequency Division Multiplexing Power Line Communication Transceivers for ITU-T G.hnem Networks.

[4] Phillips, H. 1999. "Modelling of Powerline Communication Channels." In *Proc. IEEE Int. Symp. Power Line Commun. and Its App.*, 14-21.

[5] NIST Special Publication 1108R2: *NIST Framework and Roadmap for Smart Grid Nteroperability Standards, Release 2.0*. Gaithersburg, MD: NIST.

[6] Lars, T. B., Andreas, S., and Joaquín, J. E. G. 2013. "Power Line Communications for Smart Grid Applications." *Journal of Electrical and Computer Engineering* 2013 (3), ID 712376, 16 pages.

[7] Tlich, M., Zeddam, A., Moulin, F., and Gauthier, F. 2008. "Indoor Power-Line Communications Channel Characterization up to 100 Mhz—Part I: One-Parameter Deterministic Model." *IEEE Transactions on Power Delivery* 3 (23): 1392-401.

[8] Tlich, M., Zeddam, A., Moulin, F., and Gauthier, F. 2008. "Indoor Powerline Communications Channel Characterization up to 100 Mhz-Part II: Time-Frequency Aanalysis." *IEEE Transactions on Power Delivery* 3 (23): 1402-9.

[9] Zimmermann, M., and Dostert, K. 2002. "A Multipath Model for the Powerline Channel." *IEEE Trans. Commun.* 50 (4): 553-9.

[10] José, A. C., Luis, D., Francisco, J. C., Juan, J. S. M., and José, T. E. 2011. "Performance Analysis of OFDM Modulation on Indoor Broadband PLC Channels." *URASIP Journal on Advances in Signal Processing* 33 (1):78.

[11] Hao, L., Aawatif, H., and Pierre, S. 2009. "An Information Theoretic Analysis on Indoor PLC channel Characterizations, Power Line Communications and Its Applications." *IEEE International Symposium on Power Line Communications and its Applications,* 1-6

[12] Corripio, F. J. C., Arrabal, J. A. C., del Rio, L. D., and Munoz, J. T. E. 2006. "Analysis of the Cyclic Short-Term Variation of Indoor Power Line Channels." *IEEE Journal on Selected Areas in Communications* 24 (7): 1327-38.

[13] Musolino, A., and Raugi, M. 2008. "Cyclic Short-Time Varying Channel Estimation in OFDM Power-Line Communication." *IEEE Transactions on Power Delivery* 23 (1): 157-63.

[14] Galli, S., Scaglione, A., and Wang, Z. 2010. "Power Line Communications and the Smart Grid." Presented at IEEE Int. Conf. Smart Grid Commun. (SmartGridComm), Gaithersburg, MD, USA.

[15] Chan, M., and Donaldson, R. 1986. "Attenuation of Communication Signals on Residential and Commercial Intrabuilding Power-Distribution Circuits." *IEEE Trans. Electromagn. Compat.* 28 (4): 220-9.

[16] Suguira, Y., Yamazato, T., and Katayama, M. 2008. "Measurement of Narrowband Channel Characteristics in Single-Phase Three-Wire Indoor Power-Line Channels," Presented at IEEE Int. Symp. Power Line Commun. Appl. (ISPLC), Jeju Island, Korea.

[17] Gassara, H., Rouissi, F., and Ghazel, A. 2014. "Statistical Characterization of the Indoor Low-Voltage Narrowband Power Line Communication Channel." *IEEE Transactions on Electromagnetic Compatibility* 56 (1): 123-31.